PROCEEDINGS OF THE INTERNATIONAL CONFERENCE
NANOMATERIALS: APPLICATIONS AND PROPERTIES
Vol. **3** No 1, 01NTF14(3pp) (2014)

Hydrogen Gas Response of $Zn_{1-x}Ag_xO_y$ and $Cu_{1-x}Zn_xO_y$ Nanostructured Films

V. Cretu, V. Postica, N. Ababii, V. Sontea, O. Lupan

Technical University of Moldova, 168 Stefan cel Mare Blvd, MD-2004, Chisinau, Republic of Moldova

(Received 01 July 2014; published online 29 August 2014)

Detection of hydrogen gas in industry, biomedical systems and combustion systems is important for safety reasons. Silver doping in zinc oxide and zinc doping in copper oxide were investigated to obtain improved hydrogen sensing performances for sensors. Samples were grown by chemical method and studied by X-ray diffraction, SEM and sensorial techniques. For selectivity study samples were exposed to hydrogen, methane and ethanol gases. Were found growth and annealing regimes which allow us fabrication of faster and more selective gas sensors based on $Zn_{1-x}Ag_xO_y$ nanostructured films and nanocrystallite $Cu_{1-x}Zn_xO_y$ films with respect to 100 ppm H_2.

Keywords: $Cu_{1-x}Zn_xO_y$, $Zn_{1-x}Ag_xO_y$, Chemical synthesis, Nanostructures, hydrogen, oxide, film, RTA.

PACS numbers: 81.05.DZ, 81.07.Bc

1. INTRODUCTION

Metal oxide nanoscale materials have been attracting much attention due to their unique size- and morphology-dependent physical and chemical properties [1]. It is also promising in the development of gas sensors applications and it should be expected that metal oxide nanostructures exhibit better performance than the bulk based devices [1-2]. The monitoring of H_2 and other flammable gases in industry, biomedical systems, and combustion systems is becoming important factor by increasing the requirements for sustainable and renewable energy sources. Among various types of sensors for detection such gases, chemoresistive gas sensors have been intensively investigated because of their simple usability and low cost [1-2].

Zinc oxide (ZnO) is a well known *n*-type wide band gap semiconductor (3.37 eV at 300 K for bulk material). It has been studied extensively as the main material for many modern applications, especially for sensors applications. In this regard, various synthesis methods have been explored to fabricate different nanostructures like nanowires by hydrothermal method for sensor applications [2,3], by electrodeposition for light emitting devices by europium doping [4], etc.

Cupric oxide (CuO) is a typical *p*-type semiconductor with a band gap of 1.2–1.9 eV and a monoclinic crystal structure [5-9]. Additionally, compared with other metal oxide nanostructures, such as TiO_2, ZnO, and SnO_2, copper oxide nanostructures have more interesting magnetic and superhydrophobic properties [5]. In recent years, the 'mesoporous' metal oxides, containing pores [1,6], have attracted interest for the application in gas sensors because of their high surface-to-volume ratio that can lead to improve sensitivity by the increased adsorption/reaction sites. Various works have reported about the gas-sensing properties of copper oxide, especially on quasi1D structures, like nanowires growth by surface oxidation of a Cu foil for biosensor application [7], by in situ thermal oxidation in air on Cu_2O [8], by low temperature solid-phase process [9], etc. Also were studied sensing characteristics to H_2 and C_2H_5OH of CuO mesoporous films prepared via a precursor-based ink solution route [1].

Compared to *n*-type semiconducting oxide based gas sensors, p-type oxide semiconductor gas sensors exhibit not only shortcomings but also promising potentials for practical applications [10]. In this work, were studied gas response and selectivity of $Zn_{1-x}Ag_xO_y$ and $Cu_{1-x}Zn_xO_y$ nanostructured films to different gases, namely hydrogen, methane and ethanol.

2. EXPERIMENTAL

2.1 Growth of $Zn_{1-x}Ag_xO_y$ and $Cu_{1-x}Zn_xO_y$ nanostructured films synthesized by chemical solution approach

Glass substrates were used for growth of both types of metal oxides. The cleaning process were reported in our previous work [11]. For growth $Zn_{1-x}Ag_xO_y$ nanostructured films were used the aqueous zinc complex solution approach. It comprises a mixture of zinc sulfate ($Zn(SO_4) \cdot 7H_2O$), silver nitrate ($AgNO_3$) and sodium hydroxide (NaOH) mixed until complete dissolution. The concentration of the complex solution was diluted to obtain 0.05 – 0.15 M zinc concentration for deposition by adding respective quantities of deionized (DI) water. For growth $Cu_{1-x}Zn_xO_y$ nanocrystalline films were used the aqueous copper complex solution of copper sulfate ($CuSO_4 \cdot 5H_2O$) and sodium thiosulfate ($Na_2S_2O_3$). Finally nanostructured films were exposed to different durations of rapid thermal annealing at various temperatures for 60 s**.**

2.2 Characterization

The samples of $Zn_{1-x}Ag_xO_y$ and $Cu_{1-x}Zn_xO_y$ nanostructured films were analyzed by X-ray diffraction (XRD) using a Rigaky "DB/MAX" powder diffractometer with a nickel-filtered CuKα radiation source (λ = 1.54178 Å) and a scanning rate of 0.05 °/s in the 2θ range from 30 to 90 °. The compositional analysis was carried out using energy-dispersive X-ray spectroscopy (EDX), in combination with SEM. The different characterization techniques confirmed that the nanostructured films are crystalline material.

3. RESULTS AND DISCUSSIONS

In this work were investigated gas response and selectivity to H_2 of $Zn_{1-x}Ag_xO_y$ nanostructured films (with thickness of 2.6 μm) treated by rapid thermal annealing (RTA) in air and nanocrystallite $Cu_{1-x}Zn_xO_y$ films treated by rapid thermal annealing (RTA) in furnace (with thickness of 0.95 μm). Also were investigated response (τ_r) time and recovery (τ_f) time of both type of elaborated sensors at 300 ºC operating temperature (OPT).

3.1 Chemical and Morphological Characterization

According to EDX studies the Ag content in nanostructured $Zn_{1-x}Ag_xO_y$ films was found to be at 1.3wt%Ag, while for $Cu_{1-x}Zn_xO_y$ samples about 3wt%Zn. The typical SEM image of 1.3 wt%Ag nanostructured $Zn_{1-x}Ag_xO_y$ films RTA treated at 500 ºC is represented in Figure 1a.

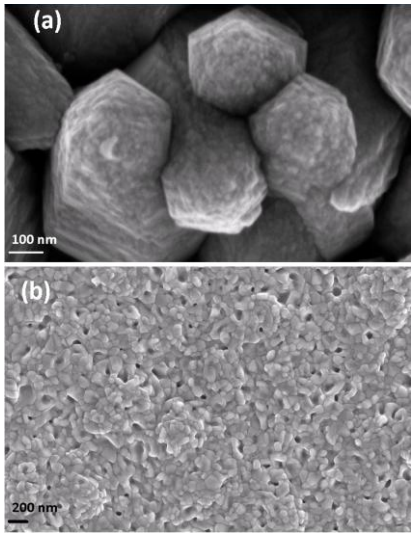

Fig. 1 – SEM images of: (a) $Zn_{1-x}Ag_xO_y$ nanostructured film RTA treated in air at 500 ºC with 2.6 μm thickness; and (b) $Cu_{1-x}Zn_xO_y$ nanocrystallite film treated RTA in furnace at 450 ºC with 0.95 μm thickness.

It can be seen that the $Zn_{1-x}Ag_xO_y$ films are composed of nanocrystallites with different diameter size (250-500 nm), while 3wt%Zn nanocrystallite $Cu_{1-x}Zn_xO_y$ films have a different structure (Fig. 1b).

3.2 Structural analysis

Fig. 2a shows the XRD pattern of as-grown and RTA treated (500 ºC for 60 s) 1.3wt%Ag nanostructured $Zn_{1-x}Ag_xO$ films recorded in the range of 30-90º with scanning step of 0.02º. All diffraction peaks can be attributed to crystalline ZnO with the hexagonal wurtzite structure (space group: $P6_3mc$ (186); a = 0.3249 nm, c = 0.5206 nm). The data are in agreement with the Joint Committee on Powder Diffraction Standards (JCPDS) card for ZnO (JCPDS 036-1451).

In Figure 2 (a) the strongest detected (hkl) peaks are at 2θ values which correspond to the following lattice planes: (100), (002), (101), (102), (110), (103), (112), (004) and (104), respectively. From the Fig. 2a was observed that diffraction peaks at the intensity of the (100), (002) and (101) were shifted by 0.1º for RTA treated sample to a lower 2θ angle value as compared with those of as-grown sample. Such lattice deformation might be result of Ag atoms incorporation in lattice of ZnO, which have greater ion radius ($r(Ag^{1+})$ = 0.126 nm) than that of Zn^{2+} ($r(Zn^{2+})$ = 0.074 nm).

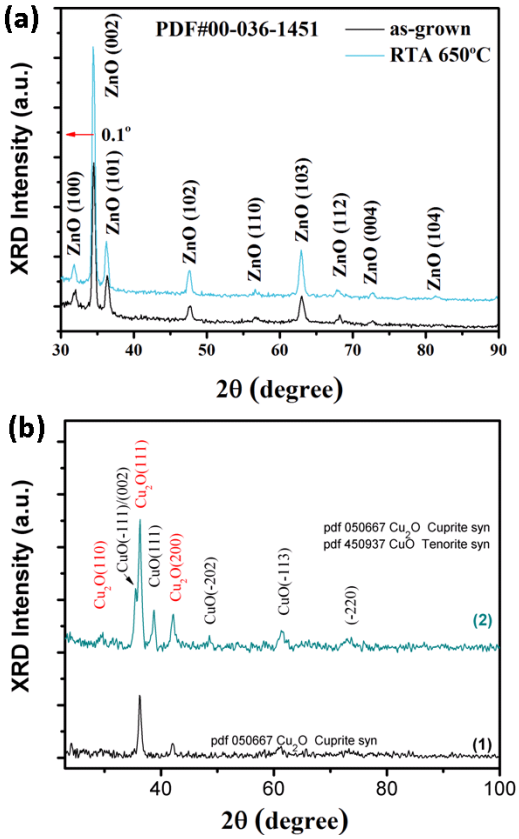

Fig. 2 – XRD patterns of: (a) the as-grown and RTA treated in air at 500 ºC $Zn_{1-x}Ag_xO_y$ nanostructured film; (b) as-grown and RTA in furnace at 450 ºC nanocrystallite $Cu_{1-x}Zn_xO_y$ film.

Fig. 2b shows the XRD pattern of as-grown and RTA treated in furnace (450 ºC for 60 s) 3wt%Zn nanostructured $Cu_{1-x}Zn_xO_y$ films recorded in the range of 23-100º with scanning step of 0.02º.

All diffraction peaks for as-grown nanocrystallite films can be attributed to cuprite (Cu_2O) phase with cubic structure (space group: Pn-3m; a = 4.2685 Å). Rapid thermal annealing in air at 450 °C with fast temperature ramp rate resulted in formation of coexisting cuprite and tenorite (CuO) phases of the deposition with monoclinic structure (space group: C_{2h}^6-C2/c; a=4.6837 Å, b=3.4226 Å, c=5.1288 Å, ß=99.54 Å).

3.3 Gas sensing studies

In order to test the gas response and selectivity to H_2 gas of $Zn_{1-x}Ag_xO_y$ and $Cu_{1-x}Zn_xO_y$ nanostructured films, the response to ethanol and CH_4 have also been investigated. The gas response of the sensors is given by the resistance change of the sensor in dry air and the resistance in the test gas as reported before [2].

There was observed no response to 100 ppm C_2H_5OH and CH_4 for of $Zn_{1-x}Ag_xO_y$ and $Cu_{1-x}Zn_xO_y$ samples at OPT 300 ºC. In Fig. 3a is demonstrated gas

response to 100 ppm H_2 versus time for nanostructured $Zn_{1-x}Ag_xO_y$ film RTA treated in air at 500 ºC and nanocrystallite $Cu_{1-x}Zn_xO_y$ film treated RTA in furnace at 450 ºC. Resistance of $Zn_{1-x}Ag_xO_y$ sample under H_2 gas exposition was decrease, so it can reach a maximum of 100% according to formula above, and demonstrate 85 % gas response, while resistance of $Cu_{1-x}Zn_xO_y$ sample was increase and demonstrate 382 % gas response.

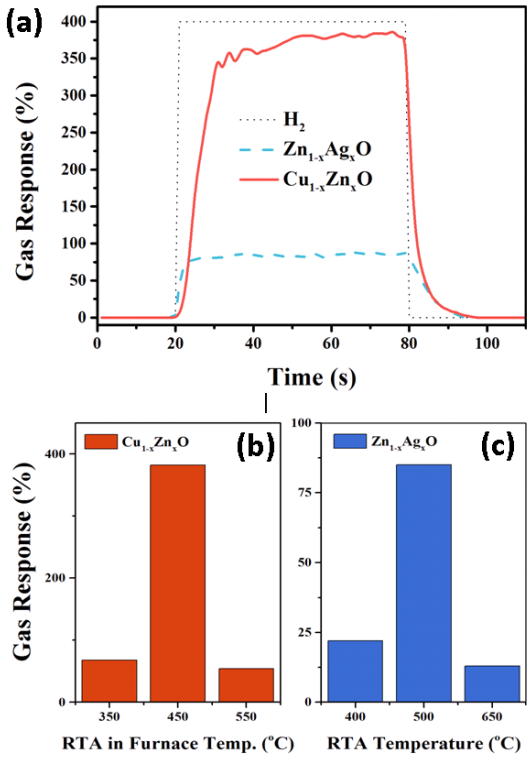

Fig. 3 – Gas response to 100 ppm H_2 of the: (a) nanostructured $Zn_{1-x}Ag_xO$ film RTA treated in air at 500 ºC with 2.6 µm thickness and nanocrystallite $Cu_{1-x}Zn_xO$ film treated RTA in furnace at 450 ºC with 0.95 µm thickness versus time to 100 ppm H_2 at OPT 300 ºC; (b) nanocrystallite $Cu_{1-x}Zn_xO$ film and (c) nanostructured $Zn_{1-x}Ag_xO$ film versus temperature of treatment type, RTA in air for $Zn_{1-x}Ag_xO$ samples after different regimes of RTA in furnace for samples, at operating temperature of 300 °C.

Also were investigated response τ_r and recovery τ_f time ($\tau = |\tau_{(90\%)} - \tau_{(10\%)}|$). From Fig. 3a it can be observed that τ_r for $Zn_{1-x}Ag_xO_y$ (τ_r = 2.8 s) sample is smaller than for $Cu_{1-x}Zn_xO_y$ (τ_r = 7.8 s) sample, while τ_f for $Cu_{1-x}Zn_xO_y$ (τ_f = 6.1 s) sample is smaller than τ_r for the same sample and smaller than τ_f for $Zn_{1-x}Ag_xO_y$ (τ_f = 11 s) sample. In Fig. 3b is presented dependence of gas response to H_2 for $Cu_{1-x}Zn_xO_y$ samples at different temperatures of RTA treatment in furnace, and can be observed that optimal temperature of treatment is 450 °C, while for $Zn_{1-x}Ag_xO_y$ samples (Fig. 3c) the optimal temperature of RTA treatment in air is 500 °C.

4. CONCLUSIONS

In summary, $Zn_{1-x}Ag_xO_y$ nanostructured films and nanocrystallite $Cu_{1-x}Zn_xO_y$ films with high crystallinity were grown on glass substrate using a chemical deposition method. SEM, EDX, and X-ray diffraction have been used to characterize the morphology, chemical composition and structure of the samples. XRD measurements indicate that synthesized $Zn_{1-x}Ag_xO$ samples are in the hexagonal phase and from XRD pattern were observed deformation in lattice by incorporation of Ag atoms, that have a higher ionic radii. XRD measurements of $Cu_{1-x}Zn_xO$ samples indicate that nanocrystalline films are synthesized in cuprite (Cu_2O) phase with cubic structure, but RTA treatment in furnace results in formation of monoclinic structure of tenorite (CuO) phase in addition to cuprite phase. From 2.6 µm thickness 1.3wt%Ag $Zn_{1-x}Ag_xO$ nanostructured films were fabricated faster sensors with 85 % gas response to 100 ppm H_2 and from 0.95 µm thickness 3wt% Zn nanocrystallite $Cu_{1-x}Zn_xO$ films were fabricated rapid sensors with 382 % gas response to 100 ppm H_2 at operating temperature of 300 °C.

AKNOWLEDGEMENTS

The authors gratefully acknowledge collaboration with Prof. Chow from UCF, USA and financial support of the STCU and ASM through Grant 09_STCU_A/5833.

REFERENCES

1. Y.H. Choi, D.H. Kim, S.H. Hong, K.S. Hong, *Sensor. Actuat. B* **178**, 395 (2013).
2. L. Chow, O. Lupan, G. Chai, H. Khallaf, L.O. Ono, B. Roldan Cuenya, I.M. Tiginyanu, V.V. Ursaki, V. Sontea, A. Schulte, *Sensor. Actuat. A* **189**, 399 (2013).
3. O. Lupan, L. Chow, L.K. Ono, B. Roldan Cuenya, G. Chai, H. Khallaf, S. Park, A. Schulte, *J. Phys. Chem. C* **114**, 12401 (2010).
4. O. Lupan, T. Papourte, B. Viana, P. Acshehoug, M. Ahmadi, B. Roldan Cuenya, Y. Rudzevich, Y. Lin, L. Chow, *Appl. Surf. Sci.* **282**, 782 (2013).
5. Q. Zhang, K. Zhang, D. Xu, G. Yang, H. Huang, F. Nie, C. Liu, S. Yang, *Prog. Mater. Sci.* **60**, 208 (2014).
6. V. Cretu, N. Ababii, V. Postica, V. Sontea, V. Trofim, S. Railean, I. Pocaznoi, O. Lupan, *II-Th Regional Workshop Health Technology Management* **1**, 72 (2014).
7. O. Akhavan, E. Ghaderi, *J. Mater. Chem.* **21**, 12935 (2011).
8. A. Li, H. Song, J. Zhou, X. Chen, S. Liu, *CrystEngComm* **15**, 8559 (2013).
9. W. Wang, Y. Zhuang, L. Li, *Mater. Lett.* **62**, 1724 (2008).
10. H.J. Kim, J.H. Lee, *Sensor. Actuat.* **192**, 607 (2014).
11. V. Postica, N. Ababii, V. Cretu, *Conferinta Stiintifica a Colaboratorilor, Doctoranzilor si Studentilor UTM*, 234 (2013).
12. L. Debbichi, M.C. Marco de Lucas, J.F. Pierson, P. Kruger, *J. Phys. Chem. C* **116**, 10232 (2012).